Supporting Information

Watase *et al.* 10.1073/pnas.0804350105

SI Text

Materials and Methods

Purkinje cell (PC) preparation. Each mouse was anesthetized with isoflurane and decapitated, and the cerebellum was dissected on ice. After removal of the meninges, the cerebella were washed twice in ice-cold high-sucrose solution (containing 30 mM Na_2SO_4, 2 mM K_2SO_4, 10 mM Hepes, 5 mM $MgCl_2$, 0.2 mM $CaCl_2$, 10 mM glucose, 180 mM sucrose, and 0.04 mM phenol red, pH 7.4 with NaOH). Each cerebellum was then minced into 10 pieces of similar size in ice-cold high-sucrose solution and transferred to a 15-ml conical tube. The pieces were allowed to settle, and the supernatant was removed. The pieces were then incubated at room temperature for 13 min in filtered papain solution [6 ml of high-sucrose solution plus 286 μl of papain slurry (Worthington), pH 7.4 with NaOH]. After papain digestion, the pieces were washed three times with 10 ml of ice-cold high-K^+ solution (82 mM Na_2SO_4, 30 mM K_2SO_4, 10 mM Hepes, 5 mM $MgCl_2$, 10 mM glucose, 1 mM EGTA and 0.04 mM phenol red, pH 7.4 with NaOH), suspended in 2 ml of high-K^+ solution and triturated 10 times with a fire-polished Pasteur pipette, followed by 10 times with a Pasteur pipette fire-polished to ½ tip diameter. The cells were plated on coverslips precoated with poly-D-lysine and laminin (BD Biosciences) in a 24-well plate (35 μl per well) containing Neurobasal complete medium (sodium pyruvate, L-glutamine, B27 and *N*-acetylcysteine). The plate was kept on ice until recording or immunostaining.

Electrophysiology. Purkinje neurons were selected based on morphology; large, pear-shaped cells lacking large processes were chosen for recording. Whole-cell currents were recorded at room temperature (20–22°C) by using an Axopatch 200B patch-clamp amplifier (Axon Instruments). Borosilicate glass capillaries were pulled in a model P-87 puller (Sutter Instruments) and heat-polished before use with a model MF-9 microforge (Narishige). Pipette resistance was $\approx$2–3 MΩ when filled with an internal solution consisting of 122 mM Cs-Asp, 10 mM Hepes, 10 mM EGTA, 5 mM $MgCl_2$, 4 mM ATP, 0.4 mM GTP, pH 7.5. The bath solution contained 167 mM TEA-Cl, 2 mM $BaCl_2$, 10 mM D-glucose, 10 mM Hepes, 0.0005 mM tetrodotoxin, pH 7.3. Series resistance was compensated electronically by $\geq$90%, and membrane capacitance (18.5 $\pm$ 0.5 pF) was corrected online; residual linear capacitive and leak currents were subtracted by the $-P/4$ method. Cells were voltage-clamped at -80 mV, and pulse depolarizations were applied at 10-s intervals. Data were passed through a 4-pole low-pass Bessel filter at 1–2 kHz, digitized at 5–10 kHz using a Digidata 1320A (Axon Instruments), and stored on a personal computer for offline analysis. Patch-clamp data were acquired and analyzed using Clampex 8.2 and Clampfit 8.2, respectively (Molecular Devices).

The Boltzmann fits of the activation and inactivation data were calculated using the equation

$$I/I_{\max} = \frac{I_2 - I_1}{1 + e^{(V - V_{0.5})/k}} + I_1 \qquad \textbf{[S1]}$$

where $I/I_{\max}$ is normalized current amplitude, V is membrane potential in mV, $V_{0.5}$ is the voltage at half-maximal $I/I_{\max}$, k is the slope factor of activation in mV/e-fold change in $I/I_{\max}$, and I_1 and I_2 are the minimum and maximum values of $I/I_{\max}$, respectively.

Immunocytochemistry. Acutely dissociated cerebellar neurons were fixed in 4% paraformaldehyde at room temperature and permeabilized with 0.5% Triton X-100 for 15 min. The cells were incubated for 1 h at room temperature with the monoclonal Tuj1 antibody (1:1,000; Covance) together with the polyclonal anti-$Ca_V2.1$ 2L1 antibody (1:200; Alomone) followed by goat anti-mouse Alexa Fluor 488 and goat anti-rabbit Alexa Fluor 546. Images were scanned using a Leica confocal microscope. To measure $Ca_V2.1$ immunoreactivity, the 488-nm channel (β-tubulin) was used to draw a region of interest around the cell body; that region of interest was then applied to the 546-nm channel. Fluorescence intensity was quantified using ImageJ 1.32j, downloaded from http://rsb.info.nih.gov/.

Immunofluorescence. For immunofluorescence, we used goat calbindin antibody (1 μg/ml), guinea pig vesicular transporter 2 (VGluT2) antibody (0.5 mg/ml), rabbit vesicular glutamate transporter 1 (VGluT1) antibody (1 μg/ml), and rabbit vesicular GABA transporter (VGAT) antibody (1 μg/ml), the specificities of which have been reported previously (1, 2). Paraformaldehyde-fixed, cerebellar sections (50 μm in thickness) were incubated with 10% normal donkey serum for 20 min, primary antibodies overnight, and Alexa 488-, Cy3- and Cy5-labeled species-specific secondary antibodies for 2 h at a dilution of 1:200 (Invitrogen; Jackson ImmunoResearch). Images were taken with a confocal laser scanning microscope (FV1000; Olympus Optical).

1. Miyazaki T, Fukaya M, Shimizu H, Watanabe M (2003) Subtype switching of vesicular glutamate transporters at parallel fibre-Purkinje cell synapses in developing mouse cerebellum. *Eur J Neurosci* 17:2563–2572.
2. Miura E, *et al.* (2006) Expression and distribution of JNK/SAPK-associated scaffold protein JSAP1 in developing and adult mouse brain. *J Neurochem* 97:1431–1446.

A

Cacna1a Exon 46 Intron 46 Exon 47

5´ ---GACAGGT--- ------AGGGCAGTAGTTCCGTCA--3´

MPI

MPc

MPII

B

MPI	AGA	CAG	GGC	AGT	AGT
	R	Q	G	S	S
MPc	AGA	CAG	TAG	TTC	CGT
	R	Q	*		
MPII	AGA	CAG	TTC	CGT	CAG
	R	Q	F	R	Q

C

Sca6 [14Q]

Cacna1a

SacII

D

I II III IV C term

$L_{I\text{-}II}$ $L_{II\text{-}III}$ $L_{III\text{-}IV}$ Ex 47

Human $Ca_V2.1$

Q_n

2L1

CT-2

A6RPT-polyQ

Fig. S1. Structural variation of $Ca_V2.1$ transcripts. (*A*) Schematic representation of alternative splicing at the boundary of intron 46/exon 47. The three splice acceptor AG sites are shown in bold letters. Transcripts and splicing events are indicated as thin lines and dashed lines, respectively. (*B*) Sequence variation of MPI, MPc, and MPII isoforms. Nucleotide and predicted amino acid sequence of the three isoforms are shown. (*C*) Alignment of sequences flanking and including the site of the CAG repeat from the wild-type *Sca6* allele and an *Sca6*[14Q] allele engineered to insert the CAG repeat into the mouse locus. Nucleotide sequences derived from human *SCA6* allele are shown in capital letters. The positions of the two SacII sites are indicated by the shaded boxes. The polyglutamine tract insertion is indicated by the single-letter code. (*D*) Diagram of mutant $Ca_V2.1$ subunit. Open bar, chimeric $Ca_V2.1$ subunit. Approximate positions of the four repeat domains (I–IV) and the C terminus (C term) are indicated on the line above. Positions of the cytoplasmic loop domains ($L_{I–II}$, $L_{II–III}$, $L_{III–IV}$) and the terminal portion encoded by exon 47 (Ex 47) are indicated below the line. The polyglutamine tract is shown as Q_n. The epitope for 2L1 is indicated as a black box within the $L_{I–II}$ domain, and arrowheads indicate positions of the two epitopes for the anti-polypeptide antibodies.

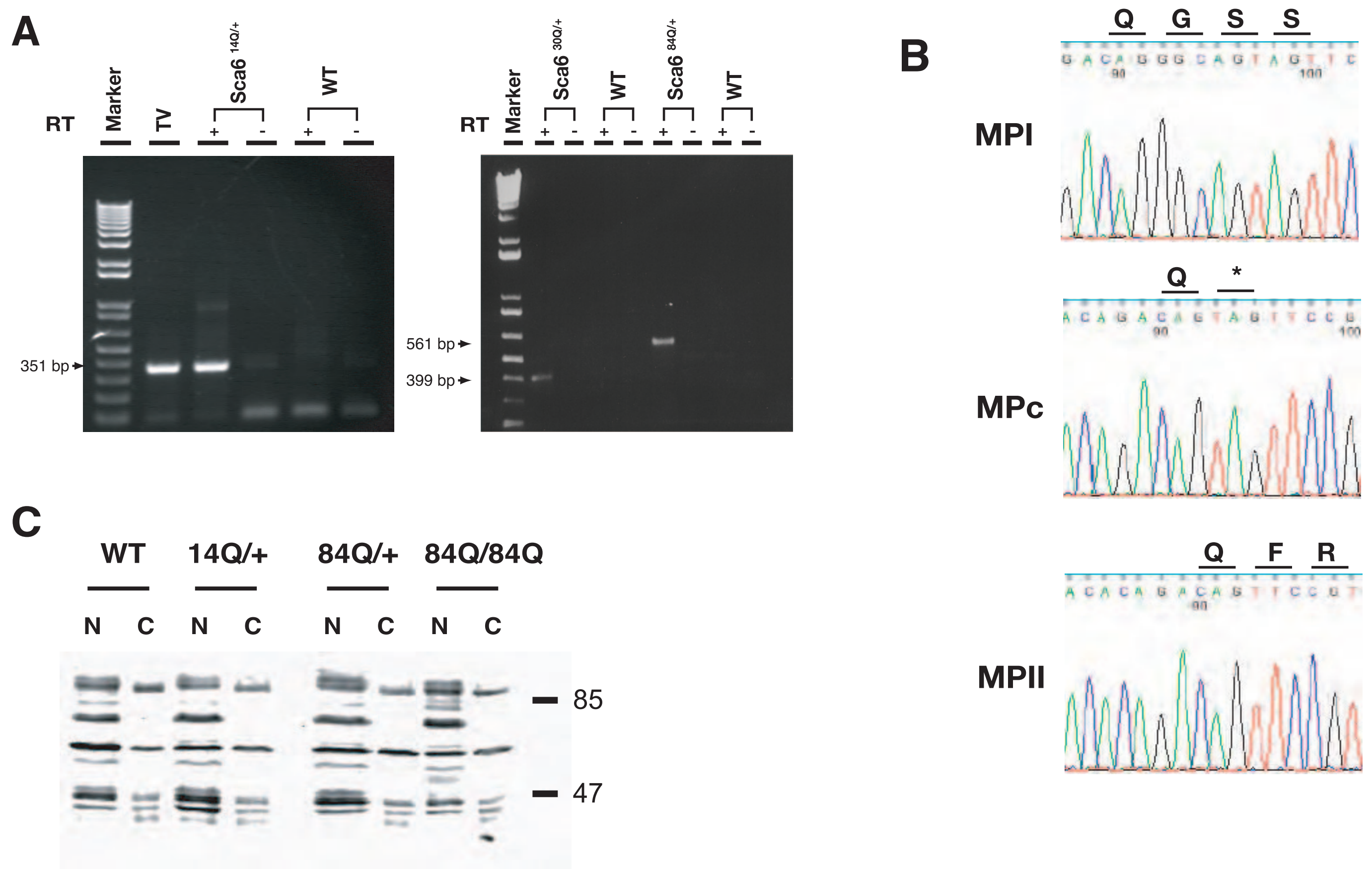

Fig. S2. Expression analysis of mutant $Ca_V2.1$ channel. (*A*) RT-PCR analysis on cerebellar RNA from 8-week-old heterozygous *Sca6* knockin (KI) animals (*Sca6*$^{14Q/+}$, *Sca6*$^{30Q/+}$, and *Sca6*$^{84Q/+}$) and their wild-type littermates (WT). The primers were designed to amplify the part of human but not mouse exon 47 that includes the tract of CAG repeats. (*Left*) Targeting vector for *Sca6*$^{14Q/+}$ (TV) was used as a positive control. (*B*) Alternative splicing at the boundary of $Ca_V2.1$ exon 46/47. cDNAs obtained from the *Sca6*$^{84Q/84Q}$ PCs were amplified and subcloned for sequencing. Electropherogram indicates the presence of the three types of alternatively spliced isoforms in the *Sca6*$^{84Q/84Q}$ PCs. (*C*) Failure to detect polyglutamine-containing C-terminal cleavage fragment in the mutant cerebella. Nuclear and cytoplasmic fractions of cerebellar lysates from 6-month-old *Sca6*$^{14Q/+}$, *Sca6*$^{84Q/+}$, and *Sca6*$^{840Q/84Q}$ KI mice and a 6-month-old WT mouse were blotted against CT-2.

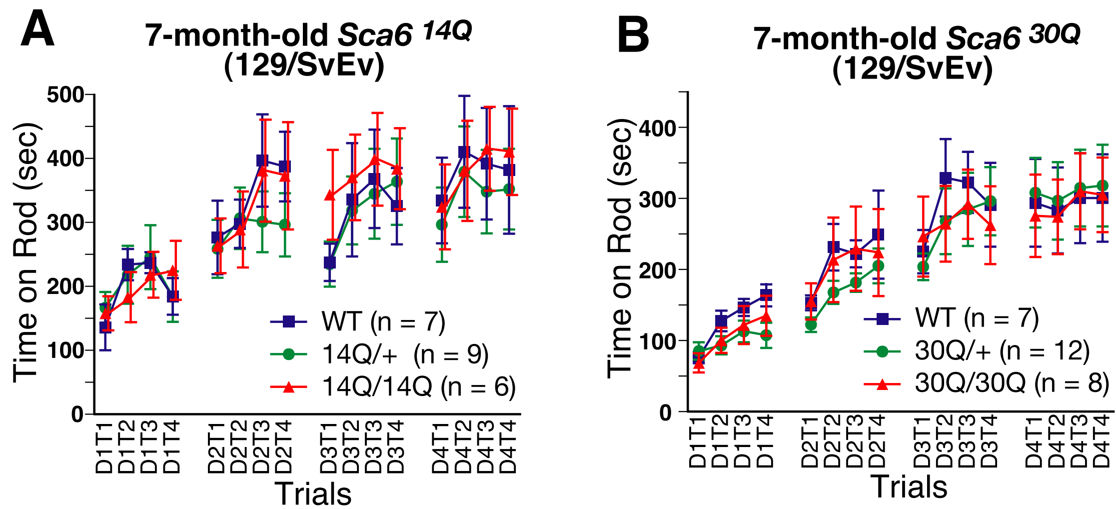

Fig. S3. Rotarod performance of 7-month-old *Sca6*$^{14Q/14Q}$ (*A*) and *Sca6*$^{30Q/30Q}$ mice (*B*) of 129/SvEv background. Mice were trained in four trials per day (T1–T4) for four days (D1–D4). Error bars indicate SEM.

Fig. S4. P/Q-type calcium channel expression is reduced in *Sca6*$^{84Q/84Q}$ Purkinje neurons. (*A*) Exemplar confocal images of Purkinje neurons stained for type III β-tubulin and $Ca_V2.1$. (*B*) Summary of immunostaining. Area was determined using the β-tubulin channel. $n = 80–100$ neurons. *, $P < 0.001$ vs. WT.

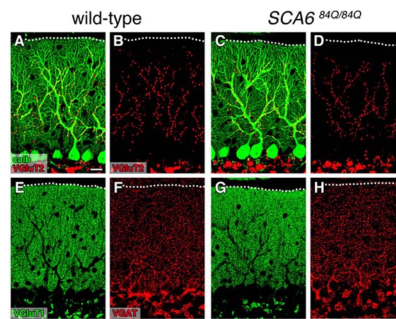

Fig. S5. Neuropathological analysis of 20-month-old *Sca6*$^{84Q/84Q}$ mouse cerebella. (*A–D*) Immunofluorescence microscopy for calbindin (green) and VGluT2 (red). Dendritic arborization of Purkinje neurons and the distribution of VGluT2-positive terminals were similar between the mutants and their wild-type littermates. (*E–H*) Immunofluorescence microscopy for VGluT1 (*E* and *G*) and VGAT (*F* and *H*) failed to show any significant changes in the distributions of VGluT1-positive terminals or of inhibitory terminals, respectively, in the mutant cerebella.